HHS Public Access

Author manuscript

Comput Diffus MRI (2014). Author manuscript; available in PMC 2015 December 12.

Published in final edited form as:

Comput Diffus MRI (2014). 2014 ; 2014: 55–64. doi:10.1007/978-3-319-11182-7_6.

Algebraic connectivity of brain networks shows patterns of segregation leading to reduced network robustness in Alzheimer's disease

Madelaine Daianu,
Imaging Genetics Center, Institute for Neuroimaging & Informatics, University of Southern California, Los Angeles, CA, USA madelaine.daianu@ini.usc.edu

Neda Jahanshad,
Imaging Genetics Center, Institute for Neuroimaging & Informatics, University of Southern California, Los Angeles, CA, USA neda.jahanshad@ini.usc.edu

Talia M. Nir,
Imaging Genetics Center, Institute for Neuroimaging & Informatics, University of Southern California, Los Angeles, CA, USA talia.nir@ini.usc.edu

Cassandra D. Leonardo,
Imaging Genetics Center, Institute for Neuroimaging & Informatics, University of Southern California, Los Angeles, CA, USA cassandra.leonardo@loni.usc.edu

Clifford R. Jack Jr.,
Department of Radiology, Mayo Clinic, Rochester, Minnesota, USA jack.clifford@mayo.edu

Michael W. Weiner,
Department of Radiology, Medicine, and Psychiatry, University of California San Francisco, CA, USA michael.weiner@ucsf.edu

Matthew A. Bernstein, and
Department of Radiology, Mayo Clinic, Rochester, Minnesota, USA mBernstein@mayo.edu

Paul M. Thompson
Imaging Genetics Center, Institute for Neuroimaging & Informatics, University of Southern California, Los Angeles, CA, USA pthomp@usc.edu

Abstract

Measures of network topology and connectivity aid the understanding of network breakdown as the brain degenerates in Alzheimer's disease (AD). We analyzed 3-Tesla diffusion-weighted images from 202 patients scanned by the Alzheimer's Disease Neuroimaging Initiative – 50 healthy controls, 72 with early- and 38 with late-stage mild cognitive impairment (eMCI/lMCI) and 42 with AD. Using whole-brain tractography, we reconstructed structural connectivity networks representing connections between pairs of cortical regions. We examined, for the first time in this context, the network's Laplacian matrix and its Fiedler value, describing the network's *algebraic connectivity*, and the Fiedler vector, used to partition a graph. We assessed algebraic connectivity and four additional supporting metrics, revealing a decrease in network robustness and increasing disarray among nodes as dementia progressed. Network components became more

disconnected and segregated, and their modularity increased. These measures are sensitive to diagnostic group differences, and may help understand the complex changes in AD.

Keywords

brain network; algebraic connectivity; Fiedler value; modularity; Alzheimer's disease

1. Introduction

Brain connectivity analyses are increasingly popular, and combine concepts from neuroscience and engineering to characterize the brain in terms of its structural and functional connections. Diffusion weighted imaging (DWI) and advanced tractography methods may offer new insights into how the brain changes in degenerative diseases such as Alzheimer's disease (AD), and its precursor, mild cognitive impairment (MCI). In addition, graph theory can be applied to study topological changes in the brain's networks using graphs – defined as a set of interconnected nodes and edges.

There is an increasing interest in analyzing the brain using graphs, which can be studied using network analysis toolboxes [1]. In a graph, network nodes are typically defined as regions of interest (ROIs) – in our case on the cortex, segmented from anatomical MRI. These nodes are linked by ‘edges’ that can be binary or weighed. However, as the field is still in its formative stages, we do not yet know which graph theoretic measures best differentiate disease states or change the most with disease progression.

Here, we applied ideas from algebraic graph theory - not previously examined in the context of AD using DWI derived measures. Specifically, we computed the second smallest eigenvalue of the Laplacian matrix (Fiedler value) for each subject to describe their algebraic connectivity – *i.e.*, how difficult it is to tear a graph apart. A Fiedler value > 0 indicates that a graph is fully connected and the higher the magnitude of the Fiedler value, the more interconnected the graph is. The Fiedler value, accompanied by a measure of link density (interconnectedness of nodes) can further describe the robustness of a graph – the denser the connections, the less vulnerable the brain network is to being disconnected. Similarly, based on the set of eigenvalues, we determined the number of disconnected network components (ROIs that do not have connections to other ROIs, or where network connections are not detected). To expand our analysis of brain connectivity, we computed more standard measures of modularity – a measure that describes the degree to which a network may be subdivided to significantly delineated groups of nodes [1,2].

To determine whether the network changes were behaviorally and clinical relevant, we related the network measures to the Mini Mental Status Examination score – a simple but widely-used test to evaluate patients and help in diagnosis of dementia. We hypothesized that with disease progression, the graph representation of the brain would become more modular (*i.e.*, segregated), reducing the density of connections among its ROIs and eventually, leading to disconnections among its nodes. We expected to see changes predominantly in the entorhinal areas and temporal cortices, areas affected first by structural atrophy in Alzheimer's disease. In diagnostic group comparisons, we also aimed to show

that the algebraic connectivity is disrupted. The overall goal of our work is to mathematically describe how the brain network changes in disease. Although all measures were sensitive to disease effects in the ADNI cohort, we found that the Fielder value was most sensitive to picking up topological effects among AD patients as well as lMCI patients.

2. Methods

2.1 Participants and diffusion-weighted brain imaging

We analyzed diffusion-weighted images (DWI) from 202 participants scanned as part of the Alzheimer's Disease Neuroimaging Initiative (ADNI). ADNI is a large multi-site longitudinal study to evaluate biomarkers of AD. **Table 1** shows the demographics of the participants included here, including age, sex, and mini-mental state exam (MMSE) scores, broken down by diagnosis. All 202 participants underwent whole-brain MRI on 3-Tesla GE Medical Systems scanners, at 16 sites across North America. Standard anatomical T1-weighted IR-FSPGR (inverse recovery fast spoiled gradient recalled echo) sequences were collected (256×256 matrix; voxel size = 1.2×1.0×1.0 mm^3; TI = 400 ms; TR = 6.984 ms; TE = 2.848 ms; flip angle = 11°) in the same session as the DWI (128×128 matrix; voxel size: 2.7×2.7×2.7 mm^3; scan time = 9 min). 46 separate images were acquired for each scan: 5 T2-weighted images with no diffusion sensitization (b_0 images) and 41 diffusion-weighted images (b = 1000 s/mm^2). Image preprocessing was performed as described previously in [3]. This was not included here due to space limitations.

2.2 NxN Connectivity Matrix Creation

We performed whole-brain tractography as described in [3]. We used a method based on the Hough transform to recover fibers, using a constant solid angle orientation distribution function to model the local diffusion propagator. Each subject's dataset contained ~10,000 useable fibers (3D curves) in total [4]. 34 cortical labels per hemisphere, as listed in the Desikan-Killiany atlas [5], were automatically extracted from all aligned T1-weighted structural MRI scans with FreeSurfer (http://surfer.nmr.mgh.harvard.edu/).

For each subject, a 68×68 connectivity matrix was created whereby each element represented the total number of fibers, in that subject, that passes through each pair of ROIs. For simplicity, all connectivity matrices were binarized to describe whether any connection was detected between a pair of cortical ROIs (marked as 1), or otherwise (marked as 0). Weighted networks will be considered in future work.

2.3 Algebraic connectivity and supporting network metrics

Algebraic graph theory is a branch of mathematics that uses linear algebra and matrix theory to study the properties of graphs [6]. In algebraic graph theory, the Laplacian matrix is used to study the *spectrum* of a graph, which is the topic of study in another branch of mathematics known as *spectral graph theory* [6]. Recently, spectral theory has been applied to study the separability of brain networks in resting-state functional MRI data from ADHD participants [8]; also, it was employed to study the altered networks in AD using magnetoencephalography (MEG) data [9]. Other applications of algebraic graph theory are in the fields of circuit design, parallel and distributive computing, data representation [10]

and the online web [11]. Here, we are the first to explore the application of algebraic graph theory to better understand the global structural changes in Alzheimer's disease using DWI derived networks.

Structural networks are usually modeled as undirected and symmetric graphs, *G(N,E)* containing a set of nodes, *N*, and edges, *E*. Here we computed an adjacency matrix for each graph, $A(G)=a_{ij}$, where a_{ij} was 1 if a connection linked a pair of nodes and 0 otherwise. Next, we computed the Laplacian matrix of graph *G* (**Fig. 1**), $L(G)=l_{ij}$, where *L(G)=D(G)-A(G). D(G)* is the *NxN* diagonal degree adjacency matrix (*i.e.*, diag(sum(*G*))). Then, the eigenvalues, λ_i, were computed on the Laplacian matrix, where $0=det(L-\lambda I)$ and *I* is an *NxN* identity matrix. In this study, we were interested in the second smallest eigenvalue, also called the Fiedler value, and its corresponding eigenvector, $\boldsymbol{x}$, computed from $(L-\lambda I)\boldsymbol{x}=0$ [10].

The magnitude of the Fiedler value describes the *algebraic connectivity* among the elements of a network; a Fiedler value of zero indicates that the network is disconnected [12]. The Fiedler value may be used in conjunction with the number of edges and nodes to further describe the robustness of a network [13]. To evaluate robustness, we also computed the number of edges in each brain network, *E*, and the link (edge) density defined as $d=2E/N(N-1)$, because a decreasing edge density may indicate decreased robustness.

Another measure obtained from the eigenvalues of *L(G)*, the number of $\lambda_i=0$, which reflects the number of disconnected components in the brain network [11]. The number of network components was further assessed with *modularity* computed using Newman's equations [2]. The algorithm efficiently defines an optimal community structure into non-overlapping sets of nodes such that the within group edges are maximized and the between-group edges are minimized. Essentially, modularity is a statistical evaluation of the degree to which the network may be subdivided to significantly delineated groups of nodes, $Q = \Sigma_{u\in M}(E_{uu} - (\Sigma_{v\in M} E_{uv})^2)$, where *M* is a nonoverlapping module that the network is subdivided into, and E_{uv} is the proportion of links that connects nodes in module *u* to nodes in modules *v* [1, 2]. If $Q < 0.3$, the community structure formed is not significant as the within-community edges are close or equal to what would be expected by chance; however, $Q \geq 0.3$ signifies significant community structures [2].

To plot the algebraic connectivity we sorted brain network nodes as a function of the Fiedler vector; components in the brain were assigned to groups based on the sorted magnitude of the eigenvector's corresponding component. This method is similar to *spectral partitioning* [7], however, in this study no partitions were added. Tools from the MIT Strategic Engineering website (http://strategic.mit.edu) were used for all calculations [11] excluding the modularity measure implemented from Newman [2] in the brain connectivity toolbox [1].

2.4 Statistical analyses

First, we assessed if the graph metrics (Fiedler value, total number of nodes, link density, the number of disconnected components and modularity) related to Mini Mental State Examination (MMSE) scores across all 202 participants using a random-effects regression,

covarying for sex and using site as a grouping variable. As we cannot assume statistical normality for the network measures, nonparametric methods may be more appropriate. We performed m=10,000 permutations of the independent variable of interest (*i.e.*, MMSE or disease status), while maintaining covariates (sex and age and imaging site) true to the subject. Next, we generated permutation-corrected p-values using the following formula: $p=(b+1)/(m+1)$, where b is the number of randomized test statistics t_{perm} found to have a greater magnitude than the observed test statistic t_{obs}. By performing 10,000 permutations, the smallest possible permutation corrected p-value is 10^{-4}, so even if the observed p-value was much less than 10^{-4}, the lowest corrected p-value was 10^{-4}.

Next, we tested if any of the graph theory metrics that closely describe algebraic connectivity (*i.e.*, Fiedler value, link density and modularity) detected group differences between controls and the diseased groups by running a random-effects regression with controls coded as 0 and diseased participants coded as 1, covarying for age and sex and using the imaging site as a random-effects grouping variable, to eliminate confounding effects of the scan site. Then, 10,000 permutations of the independent value were performed as described above.

3. Results

MMSE scores – a measure of clinical decline – were significantly related to 5 of the network measures across all 202 participants. To adjust for multiple statistical tests, the significance threshold was set to 0.05/5 when testing associations of MMSE with 5 network measures. MMSE scores declined with a decreasing Fielder value ($p_{perm}<10^{-4}$) decreasing total number of edges ($p_{perm}<10^{-4}$) and decreasing link density ($p_{perm}<10^{-4}$). Meanwhile, as hypothesized, MMSE scores declined with an increasing number of disconnected components ($p_{perm}=3.2\times10^{-3}$) in the network and increasing modularity among network communities ($p_{perm}=3.4\times10^{-4}$). These disruptions led to a less robust and inefficient distribution of the brain's network components with advancing disease, and were sorted here as a function of the eigenvectors corresponding to the Fiedler eigenvalue (**Fig. 2**). Also, brain regions that showed most frequent disconnections (0 eigenvalues) among diseased participants were those of the entorhinal, temporal and frontal poles bilaterally, in line with the sites that typically show the earliest AD pathology.

For the group comparisons, AD participants showed a significantly decreasing algebraic connectivity and a topological organization of the brain network that was different overall, relative to controls. Here, the significance threshold was set to 0.05/3, to adjust for testing 3 network metrics in the group comparison. The Fiedler value ($p_{perm}<10^{-4}$) and link density ($p_{perm}<10^{-4}$) was lower in AD, than in controls. Meanwhile, modularity increased in AD, relative to healthy elderly ($p_{perm}<10^{-4}$).

For group comparisons between lMCI and controls, the Fiedler value was the only measure to be significantly decreasing in lMCI, relative to healthy elderly (permuted p-value=0.012). No significant differences were detected between eMCI and controls; this is not surprising as this group comparison is typically the most challenging among those we tested.

The average link density was 0.360 across all healthy elderly, 0.331 in eMCI and 0.333 in lMCI participants, and 0.304 in AD. This indicates that eMCI and lMCI had an 8.2-8.8% "less" interconnected network, under this metric, while the AD patients had a 15.7% less interconnected network.

4. Discussion

This study introduces the application of algebraic connectivity, with additional supporting neural metrics, to the analysis of brain connectivity. Here, we treated the networks as sets of nodes and edges and analyzed their interconnectedness based on associations with cognitive decline scores (*i.e.*, MMSE) and diagnostic group differences. We fused all steps of analysis together and reported an overall assessment of how and where in the brain Alzheimer's strikes.

The decline in algebraic connectivity, as indicated by the decreased Fiedler values with disease progression (decreasing MMSE scores), accompanied by the reductions in the density of connections among brain regions, highlights the loss of interconnectedness within the brain network. The diseased brains may be more vulnerable to losses in connections that allow communication between cortical regions, leading to a less robust neural network, at least according to these mathematical metrics. If brain connections were to be purged (lost altogether), eMCI and lMCI brain networks would disconnect approximately 8-9% more readily than healthy networks, while AD brain networks would disconnect approximately 16% more readily than controls. Cortical regions that contributed the most to the loss of nodes were located in the entorhinal areas – regions that typically degenerate early in AD [14, 15], and the temporal pole progressing into the frontal pole in the more impaired – also supported by previous studies [14]. Disconnections in these nodes may in turn impair connected nodes, as information transfer may be reduced accordingly.

Modularity computed on the original graphs (not the Laplacian) was used to verify the goodness of component partitioning in the brain network [8]. Modularity increased with disease progression indicating that the brain networks became more segregated (formed more modular structures) with a loss in connections between modules, leading to a less efficient distribution of the network overall (**Fig. 2**). This complements the Fielder value, which defines the level of network integrity (*i.e.*, connectedness) in the brain.Modular networks were less defined in controls at an average Q=0.34, with Q=0.36 in eMCI and lMCI and Q=0.39 in AD participants – leading to readily detectable disease differences.

The Fiedler value, link density, and modularity were sensitive to group differences in eMCI, lMCI and AD, versus controls (except for the Fiedler value that did not detect differences in eMCI, relative to controls). The direction of change for all these measures indicated an overall lower interconnectness for the diseased connectomes (**Fig. 3**).

Discovering changes in brain network organizational properties allows us to understand disease progression with additional detail. Most of these network algorithms have been successfully developed and applied for non-medical applications such as online social interactions [11] and functional imaging [8, 9]; our study used these properties to study

disease progression using DWI. We found that measures such as the Fiedler value - a measure of algebraic connectivity - was the most sensitive measure to detecting differences between disease groups and controls. Supporting network metrics, such as the number of edges, link density, the number of disconnected components, and modularity, validate and strengthen the results indicating a less robust and more segregated brain with increased cognitive impairment. As a limitation, we acknowledge that future studies should compare these new metrics with standard DTI-derived measures such as FA and MD, and other non-DTI or non-imaging biomarkers of AD, to determine what added predictive value they contain. Also, for future works, weighted matrices (*i.e.*, with measures of fiber density or FA) will be used and may provide additional information about network disruptions. Overall, the network disruptions in disease are so complex that the added mathematical descriptors are likely to enhance our understanding of network dysfunction in the living brain.

Acknowledgments

Algorithm development and image analysis for this study was funded, in part, by grants to PT from the NIBIB (R01 EB008281, R01 EB008432) and by the NIA, NIBIB, NIMH, the National Library of Medicine, and the National Center for Research Resources (AG016570, AG040060, EB01651, MH097268, LM05639, RR019771 to PT). Data collection and sharing for this project was funded by ADNI (NIH Grant U01 AG024904). ADNI is funded by the National Institute on Aging, the National Institute of Biomedical Imaging and Bioengineering, and through contributions from the following: Abbott; Alzheimer's Association; Alzheimer's Drug Discovery Foundation; Amorfix Life Sciences Ltd.; AstraZeneca; Bayer HealthCare; BioClinica, Inc.; Biogen Idec Inc.; Bristol-Myers Squibb Company; Eisai Inc.; Elan Pharmaceuticals Inc.; Eli Lilly and Company; F. Hoffmann-La Roche Ltd and its affiliated company Genentech, Inc.; GE Healthcare; Innogenetics, N.V.; IXICO Ltd.; Janssen Alzheimer Immunotherapy Research & Development, LLC.; Johnson & Johnson Pharmaceutical Research & Development LLC.; Medpace, Inc.; Merck & Co., Inc.; Meso Scale Diagnostics, LLC.; Novartis Pharmaceuticals Corporation; Pfizer Inc.; Servier; Synarc Inc.; and Takeda Pharmaceutical Company. The Canadian Institutes of Health Research is providing funds to support ADNI clinical sites in Canada. Private sector contributions are facilitated by the Foundation for the National Institutes of Health. The grantee organization is the Northern California Institute for Research and Education, and the study is coordinated by the Alzheimer's Disease Cooperative Study at the University of California, San Diego. ADNI data are disseminated by the Laboratory for Neuro Imaging at the University of Southern California. Other support was also offered by NIH grants P30 AG010129 and K01 AG030514 from the National Institute of General Medical Sciences. This work was also supported in part by a Consortium grant (U54 EB020403) from the NIH Institutes contributing to the Big Data to Knowledge (BD2K) Initiative, including the NIBIB and NCI.

References

1. Rubinov M, Sporns O. Complex network measures of brain connectivity: uses and interpretations. Neuroimage. 2010; 52(3):1059–69. [PubMed: 19819337]
2. Newman ME. Fast algorithm for detecting community structure in networks. Phys Rev E Stat Nonlin Soft Matter Phys. 2004; 69(6 Pt 2):066133. [PubMed: 15244693]
3. Daianu M, Jahanshad N, Nir TM, Toga AW, Jack CR Jr. Weiner MW, Thompson PM, the Alzheimer's Disease Neuroimaging Initiative. Breakdown of Brain Connectivity between Normal Aging and Alzheimer's Disease: A Structural k-core Network Analysis. Brain Connectivity. 2013; 3(4):407–22. [PubMed: 23701292]
4. Aganj I, Lenglet C, Sapiro G, Yacoub E, Ugurbil K, Harel N. Reconstruction of the Orientation Distribution Function in Single and Multiple Shell Q-Ball Imaging within Constant Solid Angle. Magn Reson Med. 2010; 64(2):554–466. [PubMed: 20535807]
5. Desikan RS, Segonne F, Fischl B, Quinn BT, Dickerson BC, Blacker D, Buckner RL, Dale AM, Maguire RP, Hyman BT, Albert MS, Killiany RJ. An automated labeling system for subdividing the human cerebral cortex on MRI scans into gyral based regions of interest. Neuroimage. 2006; 31(3): 968–80. [PubMed: 16530430]
6. Norman, B. Algebraic Graph Theory. 2nd edn.. Cambridge University Press; Cambridge: 1993.

7. Mohar, B. The Laplacian spectrum of graphs. In: Alavi, Y.; Chartrand, G.; Oellermann, OR.; Schwenk, AJ., editors. Graph Theory, Combinatorics, and Applications. Vol. 2. Wiley; 1991. p. 1-28.

8. Bohland JW, Saperstein S, Pereira F, Rapin J, Grady L. Network, anatomical, and non-imaging measures for the prediction of ADHD diagnosis in individual subjects. Front Syst Neurosci. 2012; 6:78. doi: 10.3389/fnsys.2012.00078. [PubMed: 23267318]

9. de Haan W, van der Flier WM, Wang H, Van Mieghem PF, Scheltens P, Stam CJ. Disruption of functional brain networks in Alzheimer's disease: what can we learn from graph spectral analysis of resting-state magnetoencephalography. Brain Connect. 2012; 2(2):45–55. [PubMed: 22480296]

10. Chung FRK, Faber V, Manteuffel TA. SIAM J. Discrete Math. 1994; 7:443.

11. Bounova G, de Weck OL. Overview of metrics and their correlation patterns for multiple-metric topology analysis on heterogeneous graph ensembles. Phys Rev E. 2012; 85:016117.

12. Fiedler M. Algebraic connectivity of graphs. Czechoslovak Math. J. 1973; 23:298–305.

13. Jamakovic A, van Mieghem P. On the Robustness of Complex Networks by Using the Algebraic Connectivity. Networking, Network ad-hoc and sensor networks, wireless networks, next generation Internet. Lecture Notes in Computer Science. 2008; 4982:183–194.

14. Thompson PM, Hayashi KM, de Zubicaray G, Janke AL, Rose SE, Semple J, Herman D, Hong MS, Dittmer SS, Doddrell DM, Toga AW. Dynamics of Gray Matter Loss in Alzheimer's Disease. J Neuroscience. 2003; 23(3):994–1005. [PubMed: 12574429]

15. Devanand DP, Pradhaban G, Liu X, Khandji A, De Santi S, Segal S, Rusinek H, Pelton GH, Honig LS, Mayeux R, Stern Y, Tabert MH, de Leon MJ. Hippocampal and entorhinal atrophy in mild cognitive impairment: prediction of Alzheimer. Neurology. 2007; 68(11):828–836. [PubMed: 17353470]

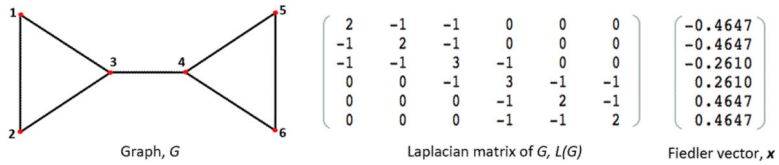

Figure 1.

Illustration of a graph *G*, its corresponding Laplacian matrix, *L(G)*, and the Fiedler vector, ***x.*** The algebraic connectivity of *G* is approximately 0.43.

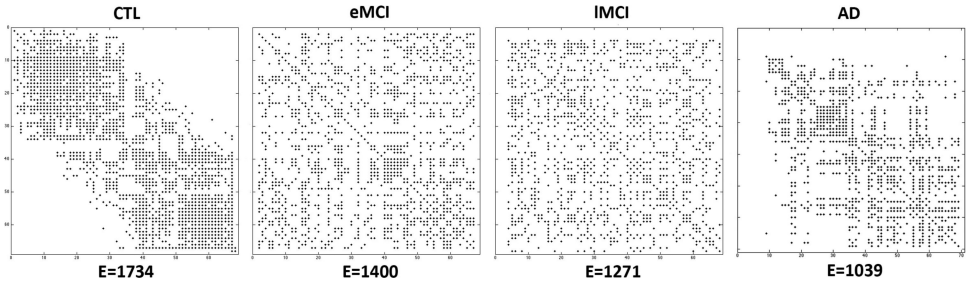

Figure 2.

Sorted connectivity matrix as a function of the sorted eigenvector, ***x***, corresponding to the Fiedler value (*i.e.*, second smallest eigenvalue) in one participant from each diagnostic group. *E* is the number of edges within each network. The plots indicate patterns of disarray with increasing numbers of disconnected components with disease progression; no completely disconnected components are shown in controls (CTL) (no zero value rows/columns, *i.e.*, missing dots), but there are 2 in eMCI, 4 in lMCI and 8 disconnected components in AD.

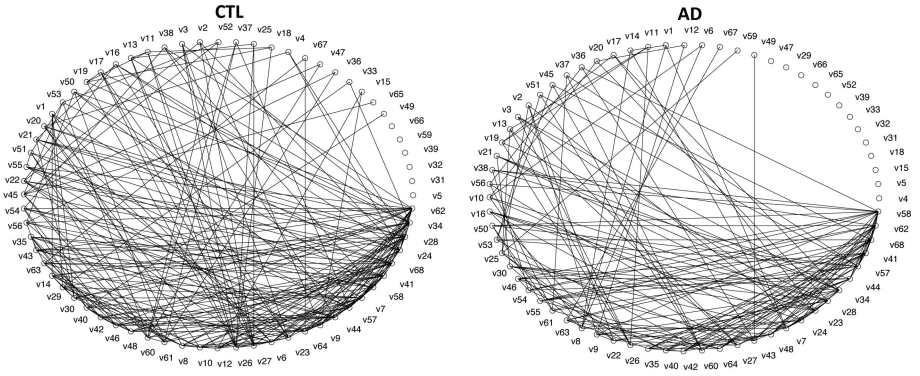

Figure 3.

Circle drawings of nodes (*v1* through *v68*) interconnected by averaged edges across 50 controls (CTL) and 42 AD participants. The loss in link (edge) density across the nodes indicates decreased interconnectedness.

Table 1

Demographic information from 50 controls, 72 eMCI, 38 lMCI and 42 AD participants scanned with diffusion MRI as part of the ADNI project. Their ages ranged from 55.2 to 90.4 years. The mean age and mini mental state exam (MMSE) scores are listed for each diagnostic group.

	Controls	eMCI	lMCI	AD	Total
N	50	72	38	42	202
Age (mean ± SD in years)	72.6 ± 6.1	72.4 ± 7.9	72.6 ± 5.6	75.5 ± 8.9	73.1 ± 7.4
MMSE (mean ± SD)	28.9 ± 1.4	28.1 ± 1.5	26.9 ± 2.1	23.3 ± 1.9	27.1 ± 2.7
Sex	22M/28F	45M/27F	25M/13F	28M/14F	120M/82F